

LARGE-SCALE VARIABILITY IN THE PROFILES OF H α AND H β IN THE SPECTRUM OF THE HERBIG B8e STAR MWC 419 AND A MODEL INTERPRETATION OF IT

A. V. Kurchakov,¹ M. A. Pogodin,² and F. K. Rspaev¹

Spectroscopic data taken with a moderate resolution spectrograph in the region of the H α and H β lines are presented for the Herbig B8e star MWC 419. The spectroscopic observations were accompanied by broad band BVR photometric measurements. The observations reveal a variability in the line profiles that is typical of Herbig Ae/Be stars with signs of a strong stellar wind. The greatest changes are observed in the region of the absorption components of the line profiles, which convert the profile from a type P CygII to P CygIII, as well as in the intensities of the central emission components. A model technique is used for quantitative interpretation of this variability and it shows that the P Cyg profile conversion of the absorption component can be explained in terms of a stellar wind model in which its distribution over latitude varies on a time scale of a few days.

Keywords: *stars: spectra: radiative transfer -- individual: MWC 419*

1. Introduction

The Be-star MWC 419 (BD+61°154, V594Cas, B8e, $V = 10^m.6$) is part of the young cluster NGC 225, which contains a T-association and a number of low-mass T Tauri objects. In 1960 it was included in Herbig's first list of Ae/Be stars [1], which are now regarded as young objects of intermediate mass (from 2 to $10 M_{\odot}$) in an evolutionary stage prior to the main sequence. Like all objects of this type, MWC 419 has an IR excess associated with the emission from a relict gas-dust disk [2].

One of the spectral peculiarities of MWC 419 is an intense emission in the H α line [3]. This line profile has a characteristic P Cyg structure, which is a sign of a dense stellar wind filling the space between the star and the observer. According to the modern view, the emission region surrounding Ae/Be Herbig stars contains an equatorial accretion disk and a stellar wind region at the higher latitudes. Here it is assumed that the axis of rotation of objects with the spectral

(1) V. G. Fesenkov Institute of Astrophysics, Almaty, Kazakhstan; e-mail: anatol@aphi.kz

(2) Main Astronomical Observatory, Russian Academy of Sciences, Pulkovo, St. Petersburg, Russia; e-mail: pogodin@gao.spb.ru

features of a stellar wind must have some sort of intermediate orientation with respect to the observer. (See the paper by Grinin and Rostopchina [4].)

In the early 1980's Finkenzeller and Mundt [3] pointed out that Herbig Ae/Be stars with P Cyg Balmer line profiles are not uniformly distributed over the entire range of spectral classes from F0 to B0, but are primarily concentrated in the range from A2 to B8. This feature of the distribution was subsequently confirmed with new observations, which made it possible to combine the Herbig Ae/Be stars with P Cyg line profiles into a special subgroup.

In the early 1990's one of the authors (Pogodin) organized a program of detailed, high resolution spectroscopic studies of selected objects in this subgroup with large telescopes at different observatories: the 2.6-m ZTSh telescope (Crimean Astrophysical Observatory, Ukraine), the 6-m BTA telescope (Special Astrophysical Observatory, Russian Academy of Sciences), the 1.4-m CAT telescope (ESO, Chile), the 1.6-m telescope at the LNA observatory (Brazil), etc. In a number of cases, the spectroscopy program was accompanied by parallel photometric and polarimetric observations. The published results of this program has been reviewed in the articles by Beskrovnaya and Pogodin [5] and Pogodin et al. [6]. The most detailed information has been obtained for the following objects: AB Aur, HD163296, HD50138, HD36112, HD31648, and HD190073. It has been found that the spectral variability of these stars has a number of general features on time scales ranging from months to hours, and can be interpreted in terms of models that assume structural changes in a circumstellar shell, along with the movement of various kinds of local inhomogeneities within it. This program and the results obtained from it are described in detail in the doctoral dissertation of Pogodin [7].

The object of this work is to obtain new observational data on and to study the features of the spectral variability of yet another little-studied Herbig Ae/Be star with signs of a stellar wind, MWC 419, and to compare our results with those reported previously for other objects in this subgroup. An attempt is also made to interpret some of the observed phenomena quantitatively using the model technique.

2. Observations

The observations were made at the high-mountain observatory at the Assy-Turgen Astrophysical Institute of the Ministry of Education and Science of the Republic of Kazakhstan, where a program of spectral studies of young Herbig Ae/Be stars and T Tau stars was begun in 2002. The observations employed a UAGS spectrograph mounted at the Cassegrain focus of the 1-m Zeiss telescope. The radiation detector was an ST-8ei CCD matrix (1530×1020 pixels), which yielded a reciprocal dispersion of 0.5 Å/pixel in the spectrograms. Observations were made in the regions of the H α and H β lines. It should be mentioned that the H β profiles were obtained first in the spectrum of MWC 419. For the characteristic 30 minute exposure time for this object, the signal/noise ratios in a single pixel at the level of the continuum spectrum were 30-50 (H α region) and 15-30 (H β region). A neon lamp was used as a comparison spectrum. All the spectra of MWC 419 that were obtained were reduced to a wavelength scale coupled to the star, with the estimated intrinsic velocity of the star relative to the solar system of -44 km/s obtained by Finkenzeller and Mundt from the position of the interstellar yellow sodium D Na I doublet lines [3].

A photometer with an ST-7 CCD matrix was attached to the same telescope at the side wall of the spectrograph (an analog of a Naismith focus) as a radiation detector for parallel *BVR* photometry of the objects under study. The

TABLE 1. Dates of Spectral Observations in the H α and H β ("+" sign) Lines

Date DMY	JD (2400000+...)	H β	Date DMY	JD (2400000+...)	H β
20.09.01	52173		09.09.02	52527	+
21.09.01	52174		03.10.02	52551	
16.10.01	52199		05.10.02	52553	+
18.10.01	52201		08.10.02	52556	
21.10.01	52204	+	09.10.02	52557	
16.11.01	52230	+	06.11.02	52585	
17.11.01	52231	+	10.11.02	52589	
19.11.01	52233	+	07.12.02	52616	
21.11.01	52235	+	06.01.03	52646	
22.11.01	52236		08.01.03	52648	
11.12.01	52255	+	02.02.03	52673	+
12.12.01	52256		29.08.03	52881	
15.01.02	52290		24.09.03	52907	
07.02.02	52313	+	28.09.03	52911	
08.02.02	52314		30.09.03	52913	
10.02.02	52316	+	19.12.03	52993	
07.09.02	52525	+	20.12.03	52994	
08.09.02	52526		19.01.04	53024	

photometric calibration was done using three comparison stars taken from catalogs of photometric standards: HD3949 (A0, $V=7^m.801$), HD3881 (A3, $V=7^m.451$) [8], and HD5996 (G8, $V=7^m.670$) [9]. The average accuracies of the determinations of the photometric parameters were: $\pm 0^m.007$ for the V magnitude, $\pm 0^m.010$ for $B-V$, and $\pm 0^m.009$ for $V-R$.

Standard programs developed at the Institute of Astrophysics were used for initial analysis of the spectral and photometric data. The apparatus, procedures for initial analysis of the data, and the first results of the research program have been published by Kurchakov and Rspaev [10,11].

Table 1 is a complete list of the dates on which spectra were obtained in the regions of the H α and H β lines and Table 2 lists the results of the BVR photometry.

3. Results of the observations

The variations of the brightness of MWC 419 in the V band and in the indices $B-V$ and $V-R$, as well as of the equivalent width of the H α (EW) line, are shown in Fig. 1. The changes in the photometric parameters were small (of amplitude $0^m.4$ for the V brightness and on the order of $0^m.1$ for the color indices). During the period from September 2002 through January 2003, a monotonic decrease in the brightness was accompanied by a significant shift to the blue

TABLE 2. Photometric Parameters Compared with the Equivalent Width of the H α Emission Line

Date (DMY)	EW (Å)	V	B - V	V - R
07.09.02	69.3	10 ^m .53	0 ^m .63	0 ^m .74
08.09.02	70.3	10.54	0.61	0.76
09.09.02	68.0	10.50	0.67	0.76
03.10.02	83.6	10.66	0.59	0.73
05.10.02	81.6	10.61	0.62	0.72
08.10.02	76.8	10.69	0.60	074
09.10.02	69.8			
06.11.02	82.4	10.60	0.60	0.73
10.11.02	78.9	10.62	0.60	0.72
07.12.02	66.8	10.76	0.59	0.68
06.01.03	67.7	10.80		0.71
08.01.03	57.4	10.46	0.66	0.75
02.02.03	71.7	10.55	0.63	0.75
29.08.03	79.2	10.62		0.64
24.09.03	86.3	10.68	0.59	0.64
28.09.03	75.4	10.66	0.64	0.62
30.09.03	69.0	10.60	0.62	0.66
19.12.03	63.9	10.61	0.62	0.62
20.12.03	66.3	10.67	0.61	0.64
19.01.04	65.6	10.68	0.62	0.64

for this object, which was observed in both of the color indices. This effect is usually observed in UX Ori type variables -- Herbig Ae/Be stars, whose disks are visible from the edge. (See, in particular, the paper by Grinin et al. [12]) It is related to the fact that a dust inhomogeneity, rotating in a plane close to the equator, may obscure a significant portion of the stellar disk and the inner region of the shell from the observer. Then the contribution of scattered radiation from the circumstellar dust to the overall emission becomes greater, thereby making the color indices "bluer." But this effect begins to be seen only for very strong brightness attenuation. It should also be accompanied by an increase in the equivalent widths of the emission lines, since the more extended gas shell is less shielded than the star itself by the dust cloud. (See Grinin et al. [13]) In the case of MWC 419, however, none of these effects were observed. The statistical significance of the slight "bluing" of the object is low (10 or fewer measurements) and at this stage we cannot say for sure that this effect is real. Our photometric measurements agree with photometric results for MWC 419 obtained in the 1980's by Shevchenko's group at the Maidanak Observatory [14], who characterized the observed variability as "small scale quasiperiodic variations in brightness on which some irregular oscillations are superimposed," as well as with the

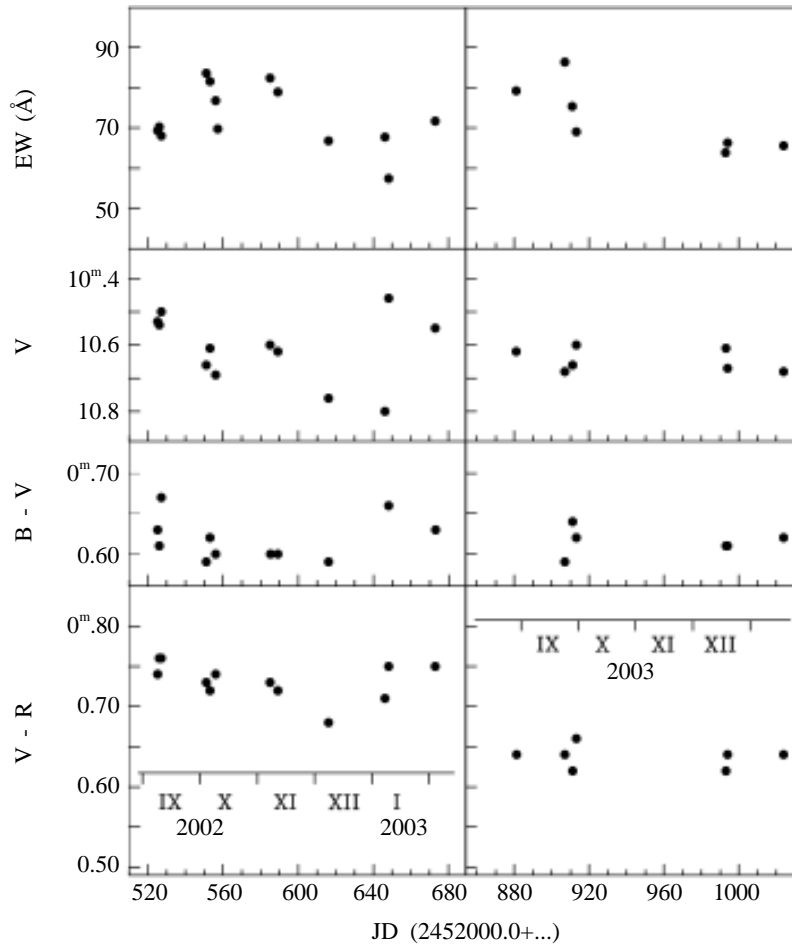


Fig. 1. Variations in the V band brightness and the color indices $B-V$ and $V-R$ of MWC 419 compared with the variation in the equivalent width (EW) of the $H\alpha$ emission line.

later conclusion of Fernández [15] who concluded that this object has no regular photometric variability that depends on wavelength. The absence of large-scale photometric variability is indicative of a small or intermediate slope of the axis of rotation of the object to the line of sight. This is to be expected for a Herbig Ae/Be star with P Cyg Balmer line profiles [4].

Our spectral observations confirm the existence of large-scale variations in the $H\alpha$ and $H\beta$ line profiles in the spectrum of MWC 419. They occur on a time scale of days to months. Typical examples of this variation for the $H\alpha$ line are illustrated in Fig. 2. In the different frames of this figure it can be seen that strong variations are observed in all parts of the line profile, including the blue absorption component, as well as the emission at the line center and in its red wing.

The variability of the absorption component may be characterized as an episodic phenomenon or as the vanishing of additional emission in the blue edge of this feature, which converts the general type of profile from P CygII into P CygIII (according to the classification by Beals [16]). In some cases, additional emission shows up right in the middle of the absorption component, leading to a more complicated profile shape with two absorption features (Fig. 2, frames

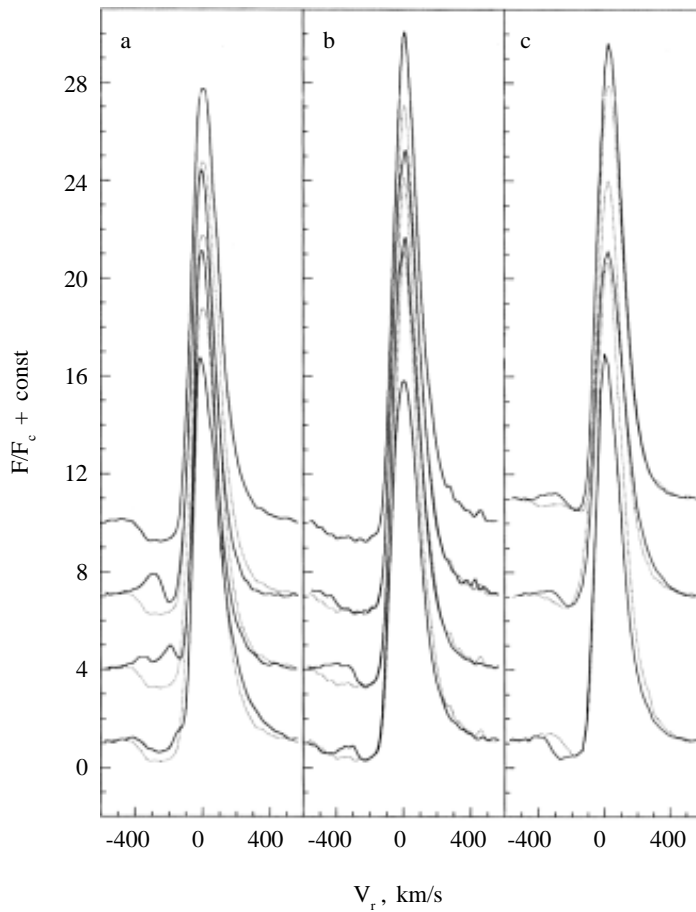


Fig. 2. Typical variations in the normalized profile of the $H\alpha$ line in the spectrum of MWC 419 over different time scales. (a) 4 profiles, from top to bottom, obtained on the successive dates Nov.10, 2002, Dec. 7, 2002, Jan. 6, 2003, and Feb. 2, 2003. The first profile is also shown as dotted curves for comparison with the others. (b) The same as in frame (a) but for spectra obtained on Oct. 3, 5, 8, and 9, 2002. (c) 3 pairs of profiles observed in successive seasons: Nov. 16 and 21, 2001, Feb. 7 and 10, 2002, and Dec. 19 and 20, 2003. The first profile of each pair is plotted as a dotted curve.

a and b). This kind of variability is typical for Herbig Ae/Be stars in this subgroup. In particular, complicated "double" P Cyg profiles of the $H\alpha$ line have been observed in the Herbig A0/A2e star HD 163296. (See Beskrovnaya et al. [17])

At various times three types of models have been proposed for explaining these variations in the profile of the absorption component:

1. A latitudinal redistribution of the density of outflowing matter (Pogodin [18]).
2. Motion of dense, rotating azimuthal inhomogeneities in a stellar wind within the space between the star and the observer (Beskrovnaya et al. [19]).
3. Kinematic changes in the region of a stellar wind associated with the formation, in it, of a solid rotation zone

caused by a strengthening of the magnetic field that controls the outflow process (Mihalas and Conti [20], Pogodin [21]).

In this paper we try to provide a quantitative interpretation of some episodes of the spectral variability of MWC 419 which we have observed in terms of the hypothesis of a latitudinal redistribution of the density of its stellar wind. A first attempt at an interpretation of this sort was made by Pogodin [18] in the early 1990's to explain the episodic disappearance of P Cyg structures in the H α and H β profiles in the spectrum of AB Aur observed in 1988. The hypothetical changes in the density of the wind at different latitudes are related to the assumption that when the accretion disk and magnetosphere of a star interact, a global magnetic field with a complex structure develops which then controls the stellar wind, accelerating it along the open field lines and forming its spatial structure. When the disk accretion regime changes, the configuration of the magnetic field may also change and, thereby, the latitudinal structure of the wind. It has now been proved directly that magnetic fields on the order of 100 G exist at the base of the stellar wind in Herbig Ae/Be stars (Hubrig et al. [22]).

4. Differential model technique

Constructing a general physical model of the circumstellar medium surrounding a Herbig Ae/Be star is currently a rather difficult task. The main difficulty is that we do not know the specific physical processes controlling energy exchange in the shell and, especially, in its interior, in the region where it interacts with the star. This is substantially due to the fact that there is insufficient information on the magnetic fields of the star itself and in its shell. This limits the possibility of physically modelling the circumstellar medium surrounding a Herbig Ae/Be star and, in particular, of applying MHD calculations to that region.

In a number of cases, phenomenological modelling, where certain physical characteristics, such as the electron temperature distribution in the shell, are specified as parameters of the model, has been effective. Successful models of the circumstellar disks of UX Ori type variables, where the radiation from the disk predominates, are well known. (See Tambovtseva et al. [23]) However, in cases where the wind plays a significant role in forming the circumstellar emission the problem of constructing a general model for the shell remains quite complicated. A complete description of the structural features of a multicomponent shell, including an equatorial disk and wind that is latitudinally nonuniform, requires the introduction of too many free model parameters. It would be impossible to determine all of these parameters uniquely with the limited amount of information obtained directly from observations.

Nevertheless, despite these difficulties, there is a possibility of using the model technique for quantitative interpretation of phenomena taking place in a circumstellar medium with a very complicated structure. Here we are speaking of the so-called differential model technique, which essentially involves modelling, not the entire shell as a whole, but only part of it, a limited spatial region (referred to below as the "active region") within which changes take place that can be responsible for the observed spectral variability. This turns out to be possible because the large velocity gradients of the large scale motions typical of the shells of Herbig Ae/Be stars ensure that the interaction between the radiation in spectral lines and the matter in different parts of the shell is local in character (Sobolev [24]). For each point in a line profile it is then possible to localize a spatial region in the circumstellar gas where the emission in the line at that point in its profile has been formed.

The model procedure as such is based on a comparison of observed and theoretical differential line profiles constructed as the difference of two individual profiles corresponding to different observation dates, the discrepancy between which also illustrates the variability that is being studied.

All of our calculations were done using a computer program that has been developed and described in detail by Pogodin [25,26]. The free parameters of the model, the basis of the program, are the distribution of the electron temperature distribution T_e , the density N of hydrogen atoms, and the velocity vector V of the large scale motions in the space containing the circumstellar gas. In the first step, the program calculates the spatial distribution of hydrogen atoms in different energy levels and the source functions for the hydrogen lines based on Sobolev's probabilistic method [24]. In the next step, theoretical profiles of the hydrogen lines of the radiation that reaches the observer are calculated by numerical integration over the entire volume of the shell, in accordance with the exact equations for radiative transport in spectral lines.

5. Choice of the "active region" model

Of all the episodes of large scale spectral variability observed in MWC 419 during the observation period, we have chosen two: (a) the conversion of P CygII H α and H β profiles into P CygIII profiles with a simultaneous increase in the central emission in the lines (the season from September 16 through November 21, 2001) and (b) the same kind of change in the profiles, observed from February 7 through 10, 2002, but accompanied by a drop in the intensity in the line centers. These episodes were chosen because:

1. On these dates observations were made of H and not just H α , which doubled the number of parameters derived directly from the observations.
2. The variability observed on these dates was fairly unambiguous, so that it could be interpreted with a simpler model (i.e., with a smaller number of model parameters).
3. In both seasons a variability was observed over small intervals of time (3-5 days). Because of this there was more reason to assume that during such a short time many of the parameters of the shell should have stayed constant. This offered the possibility of further simplifying the model.

The immediate object of our model interpretation were the differential profiles of the H α and H β lines constructed for the two seasons (November 2001 and February 2002) by subtracting the individual profile obtained on the last date from the profile obtained at the beginning of the season. (See Fig. 3, below.) Our task was to compare the theoretical and observed differential profiles and, by varying the model parameters, obtain the best agreement between these profiles, primarily in the regions of (a) the absorption components and (b) the central intensities of the emission components.

In order to correctly isolate the active region of the shell, it was necessary to understand specifically which latitudinal redistributions of the stellar wind must take place in order for the P CygII line profiles to be transformed into P CygIII profiles. The calculations show that if the wind region is compressed toward the equatorial disk and the space between the star and the observer is free of dense, outflowing gas, then a simple emission profile will be observed with no signs of a P Cyg structure. If the wind zone spread widely into high latitudes and occupies the entire region along the line of sight between the star and the observer, then the line profile will be of type P CygII [18]. The following three

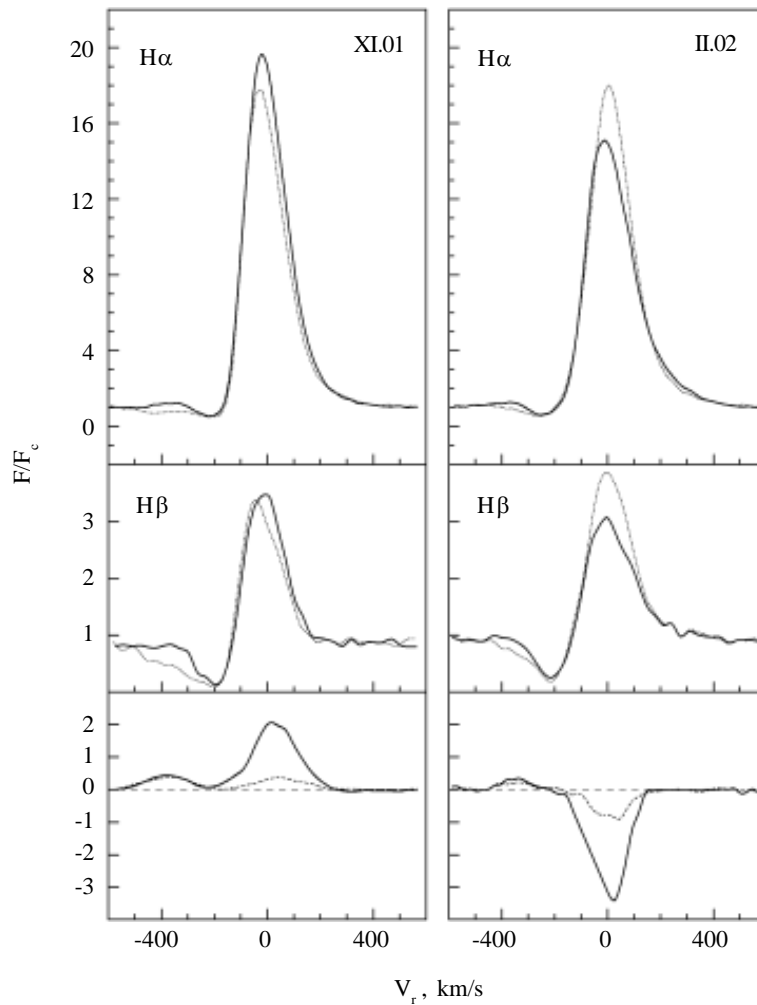


Fig. 3. Changes in the $H\alpha$ and $H\beta$ profiles observed in the spectrum of MWC 419 from November 16 through 21, 2001 and from February 7 through 10, 2002. The first profile of each pair is plotted as a dotted curve. The lower frames of the figure show the differential profiles of $H\alpha$ (smooth curves) and $H\beta$ (dotted curves) constructed for the two seasons by subtracting the first profile from the second, smoothed over a window 3 pixels wide. The dashed lines indicate the position of the zero on the F/F_c scale.

assumptions are necessary in order to explain the formation of a P CygIII profile: (a) the outer boundary of the wind zone spreads further ("flares") into the region of higher latitudes as it moves away from the star, (b) this boundary is positioned so that the space between the star and the observer is filled by outflowing matter only at large distances from the star, and (c) the outflow velocity of the wind initially increases out to a certain distance from the star as long the mechanism for accelerating it is acting and then decreases with distance in accordance with Kepler's law [7]. This last assumption (c) is physically justified, since one of the main mechanisms for acceleration of the wind in Herbig Ae/Be stars is now recognized to be the magnetic centrifuge, whose efficiency increases with distance from the star. The existing observational data also imply that lines whose widths are determined by the velocity field and are formed in a distant part of

the stellar wind (such as the Na D doublet) are narrower than those lines, such as H α and H β which are formed throughout the entire shell [3]. Under the conditions enumerated above, the wind begins to shield a star from the observer only for stars that are sufficiently distant that their velocity is substantially below the maximum. Thus, the high velocity portion of the wind will not lie on the line of sight between the star and observer, who will see a P Cyg line profile, but with an additional emission in the region of large negative velocities (a P CygIII type profile). The additional emission effect can also be enhanced by electronic scattering of the radiation in the line and increased emission in the line wings during reradiation in the wings of the profile of the absorption coefficient of the hydrogen atom if the electron density in the shell is high enough [26].

To summarize, for our model calculations we isolated a local active region in the stellar wind in accordance with the following criteria:

1. It was assumed that the active region intersects (at least partially) the line of sight and is symmetric with respect to the axis of rotation of the star, which is inclined to the line of sight by some intermediate angle i . For concreteness, all our calculations were done with $i = 45^\circ$.

2. The distributions of the temperature T_e , the density N , and outflow velocity V_p inside the active region are independent of the latitude φ .

3. The inner boundaries of the active region (i.e., from the low latitude side on both sides of the equatorial disk) correspond to latitude φ_1 .

4. The outer boundaries of the region are "concave," i.e., its position along the latitude φ_2 increases with distance. The dependence of φ_2 on distance r varies in time and the active zone can sometimes fully overlap the space between the star and the observer and sometimes be entirely absent from it.

5. We used the following approximation formulas for the radial velocity V_r and rotational velocity V_{rot} of the stellar wind inside the active region, which, for simplicity, is assumed to be flowing directly out of the star:

$$V_r(r) = V_o (r/R_o)^{0.5}, \quad \text{if } r \leq r_a, \quad (1)$$

$$V_r(r) = V_m (r_a/r)^{0.5}, \quad \text{if } r \geq r_a, \quad (2)$$

where $V_m = V_o (r_a/R_o)^{0.5} = 450$ km/s was determined from the maximum width of the observed emission profiles of the H α and H β lines, and

$$V_{rot}(r) = U_o (\rho/R_o), \quad \text{if } r \leq r_a, \quad (3)$$

$$V_{rot}(r) = U_m (\rho r_a/r^2), \quad \text{if } r \geq r_a, \quad (4)$$

where ρ is the modulus of the projection of the radius vector \mathbf{r} on the equatorial plane and $U_m = U_o (r_a/R_o)$, while $U_o = 80$ km/s, determined from the conditions $V \sin i = 55$ km/s [27] and $i = 45^\circ$. The parameter r_a characterizes the inner boundary of the region where the hypothetical magnetic field influences the kinetics of the wind.

The distribution of the hydrogen atoms density was calculated from the condition that the mass of the outflowing gas is conserved:

$$N(r) = N_o R_o^2 V_o [r^2 V(r)]^{-1} \Phi(r), \quad (5)$$

where $\Phi(r)$ is a coefficient that takes into account the "concavity" of the outer boundary of the active region. It is defined

so that $\Phi(r)r^2/R_0^2$ equals the ratio of the areas of the intersection of the active zone by spheres with radii of R_0 and r , respectively, whose centers coincide with the center of the star. If there is no "concavity" of the outer boundary, then $\Phi(r)=1$, while if it is concave, $\Phi(r)<1$.

In order for the model to be kinematically consistent, it is also necessary to introduce a hypothetical latitudinal velocity $V_\varphi(\mathbf{r})$ of the gas. This velocity is directed along the meridian toward increasing latitude and creates the "concavity" of the outer boundary of the active zone.

It was possible to simplify the model considerably for the analysis of the temperature situation in the circumstellar gas. Test calculations for isothermal shells with Te in the range from 5000 to 20000 K showed that the theoretical $H\alpha$ and $H\beta$ profiles depend weakly on Te as long as the gas remains ionized ($N^+/N_1 \gg 1$). In regions of the gas where the ratio N^+/N_1 approaches 1, the line emission falls off sharply. This allowed us to specify a constant temperature within the entire shell ($T_e=10000$ K) and introduce the model parameter r_m as the outer boundary of the shell corresponding to the distance where the gas ceases to be ionized.

6. Sensitivity of the theoretical differential profiles to changes in the input parameters of the model

Although the active region singled out here is just a limited portion of the whole shell, its description still requires too many model parameters for it to be used for unique quantitative estimates.

Thus, the next step in our study was an attempt to reduce the number of model parameters, by eliminating from the analysis those parameters to which the computational results are insensitive.

We examined the theoretical differential profile given by the difference between the two individual profiles calculated for two positions of the outer boundary of the active region: (a) the line of sight intersects this boundary at a distance ρ_0 from the star's center (Fig. 4a) and (b) the active region completely fills the space between the star and the

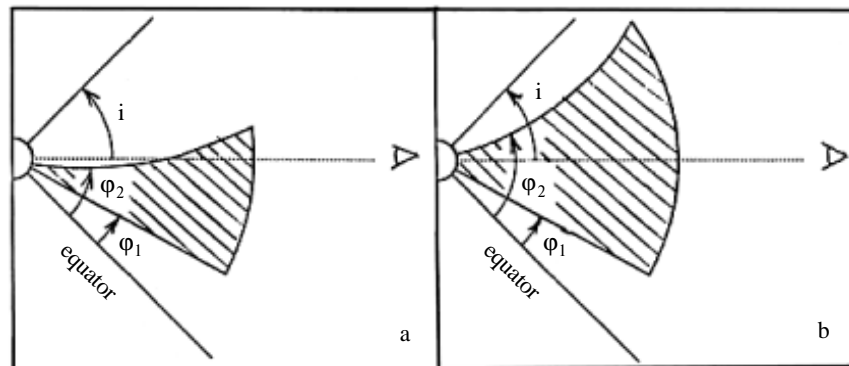


Fig. 4. Geometric model of the active region of the stellar wind projected onto the plane passing through the axis of rotation and the line of sight. The figure shows only one fragment of the projection intersecting the line of sight along the path from the star to the observer. Two cases are illustrated: (a) outer boundary of the active region intersecting the line of sight and (b) the gas flowing out within the active region filling all of the space between the star and the observer.

observer (Fig. 4b). We also assumed that the parameter $\Phi(r)$, which determines how the density falls off with distance (Eq. (5)), is the same in both cases. The subsequent analysis showed that the different parts of the computed differential profile are sensitive to the model parameters in different ways. Thus, we examined two separate components of the profile: component A, corresponding to the region of blue P Cyg absorption and component E, which is formed in the region of the maximum intensity of the emission peak.

A series of test calculations (more than 1000 variants) showed that:

1. The presence of an equatorial disk in the shell or a stellar wind outside the active region has no influence on either of the components (A or E) of the theoretical differential profile.
2. Both components (A and E) are insensitive to the presence of circumstellar gas in the active region at azimuths away from the line of sight (i.e., that do not shield the star from the observer).
3. Both components (A and E) are insensitive to a change in the position of the inner boundary φ_1 of the region, if $\text{tg}\varphi_1 \leq 0.5$, and to a change in the outer boundary $\varphi_2(r)$, if $\text{tg}\varphi_2(r) \geq 1.5$.
4. If the outer boundary of the region intersects the line of sight at a distance ρ_o from the star's center, then component A is sensitive only to the value of ρ_o . The second component E depends strongly on the form of the outer boundary, since the dependence $\varphi(r)$ determines the character of the fall in density $N(r)$ with distance in accordance with the conservation of mass (Eq. (5)).
5. Including an additional latitudinal velocity $V_\varphi(\mathbf{r})$ in the kinematics of the wind has no effect on the A and E components of the differential profile. In the calculations we examined various test functions $V_\varphi(\mathbf{r})$ and studied how they influence both the average gradients of the velocity of the large-scale motion and the line profiles.
6. The initial density N_o and the outer radius r_m of the active region have a strong influence on the E component, but a fairly weak one on the A component.
7. The parameter r_a , which determines the radius over which the magnetic field affects the kinematics of the wind, has a significant effect on both components (A and E) of the differential profile.

Therefore, the A component, which is formed in the region of the blue P Cyg absorption, depends on just two of the model parameters, ρ_o and r_a . This means that we are fully justified in using the model technique for determining these parameters in the observed stellar wind. Component E, which corresponds to the region of the emission maximum of the line profile, depends on the rate of outflow of gas in the active region, on the spatial distribution of its density, and on the outer radius of the region, that is, on the parameters N_o , r_m , $\varphi_2(r)$, and r_a .

Since there are too many parameters, we cannot use component E for a unique quantitative interpretation of the observational data.

7. Model interpretation of the differential profiles in the region of the blue P Cyg absorption

As noted in the preceding section, the differential profiles of the H α and H β lines in the P Cyg absorption region (the so-called A component) can be described quite completely using only two of the model parameters ρ_o and r_a . Thus, a simplified model of the active region with a limited number of initial parameters, some of them specified arbitrarily,

was adequate for modelling these components.

Figure 5 illustrates a family of theoretical A components calculated with a model assuming that: (a) $\text{tg}\varphi_1 = 0.2$, (b) $\Phi(r)=1$ for all r , and (c) an outer boundary of the latitudinal boundary of the active region, φ_2 , of the simple linear form

$$\text{tg}\varphi_2 = 0.4[1 + 0.2 a_1 (r/R_o)]. \quad (6)$$

The parameter a_1 in Eq. (6) characterizes the degree of curvature of the outer latitudinal boundary. It is uniquely related to the parameter ρ_o : when $r = \rho_o$, the corresponding value of a_1 ensures that $\text{tg}\varphi_2 = 1$.

The family of theoretical A components shown in Fig. 5 was calculated for $r_a = R_o, 2R_o$ and $3R_o$, and $a_1 = 1, 2, 3$, and 4. Here the differential profiles were constructed as the difference between the individual H α and H β profiles calculated for a given value of a_1 and the individual profiles of the same lines characterizing the state of the active region when the wind completely fills the space between the star and the observer but with the same dependence of $\Phi(r)$ on the distance r (Fig. 4b).

A comparison of the theoretical A profiles with the observed profiles showed that the best agreement is attained for the following values of the model parameters: (a) $r_a = 2.8 \pm 0.2 R_o$, $a_1 = 1.7 \pm 0.3$ ($\rho_o = 4.4 \pm 0.7 R_o$) for the spectra of November 2001 and (b) $r_a = 2.2 \pm 0.1 R_o$, $a_1 = 3.5 \pm 0.5$ ($\rho_o = 2.1 \pm 0.3 R_o$) for the season of February 2001. The observed A profiles of the H α and H β lines obtained in the two observational seasons are also shown in Fig. 5 for comparison with the theoretical profiles.

8. Estimate of the rate of outflow of mass in the active zone of the stellar wind

Our study of the sensitivity of the theoretical differential profiles to the various model parameters showed that the E component, which characterizes the variations in the central intensity of the individual profiles in the region of maximum emission, depends strongly on the parameters r_a , $\varphi_2(r)$, N_o , and r_m . (See Section 5.) The value of r_a was determined fairly uniquely from the A components of the differential profiles of H α and H β observed in the spectrum of MWC 419 in November 2001 and February 2002. (See Section 6.)

We do not have much information on the exact dependence $\varphi_2(r)$. In the preceding section we only estimated the distance from the star at which the outer latitudinal boundary of the active region should intersect the line of sight (the parameter ρ_o). But the specific physical processes responsible for the latitudinal "stretching" of the active zone of the wind with increasing distance from the star are still unknown. The lack of knowledge of the exact character of the distribution $V_\varphi(\mathbf{r})$ of the latitudinal velocity and, therefore, of φ_2 , is the main obstacle in the way of an unambiguous interpretation of the observed E components of the H α and H β lines in the spectrum of this object.

Nevertheless, we have tried to examine two fundamental questions:

1. Are changes in the parameters of the wind within the active region alone sufficient to explain the observed variability in the H α and H β line profiles in the region of their emission maxima?
2. What rate of loss of mass is to be expected inside the active zone and what sort of changes can it undergo on the time scale of the spectral variability being studied here (a few days)?

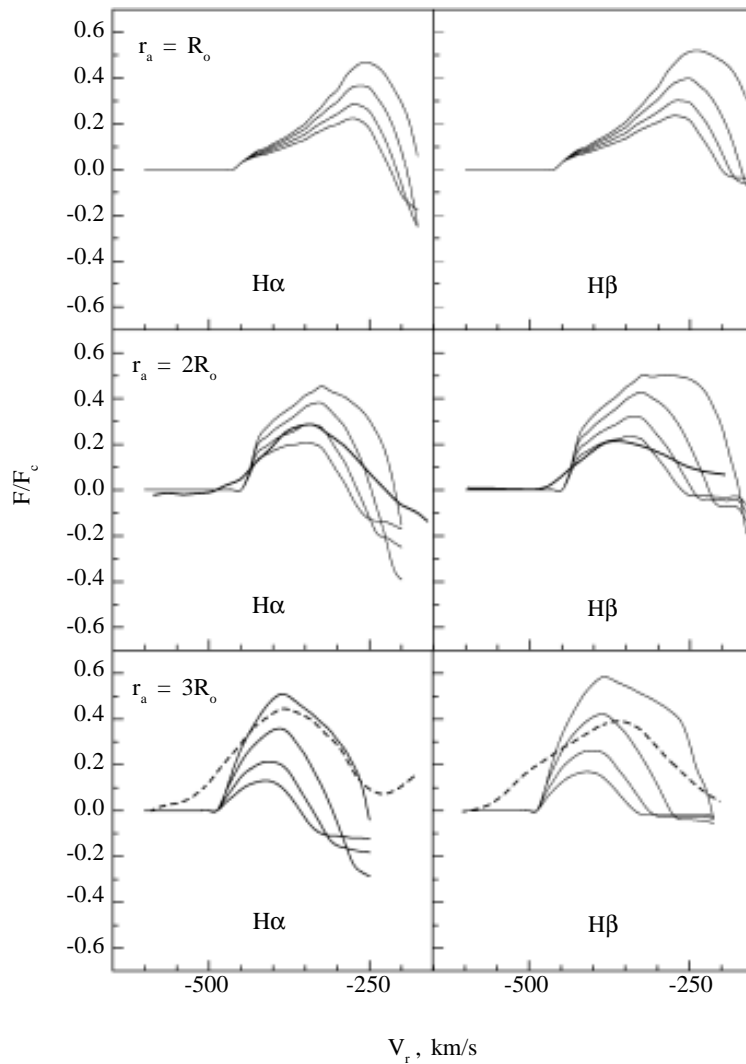


Fig. 5. A family of theoretical differential profiles of the H and H lines in the region of the absorption P Cyg component constructed for $r_a = R_o, 2R_o$ and $3R_o$, and $a_1 = 1, 2, 3$ and 4 (from top to bottom in each frame of the figure). A profile corresponding to the case of complete filling of the space between the star and the observer by the stellar wind was used as the subtrahend profile. Observed differential profiles are shown for comparison: thick dashed curves for the season of Nov. 2001 and thick smooth curves for the season of Feb. 2002.

Our test calculations were carried out in several steps, in the course of which the results for different forms of $\phi_2(r)$ were analyzed.

Ultimately, it was found that:

1. The variability in the central intensities of the H α and H β profiles observed in the spectrum of MWC 419 in both November 2001 and February 2002 can be explained in terms of the above model of an active region in the stellar

wind if: (a) $\phi_1 \leq 0.1$ and (b) ϕ_2 increases with distance no more rapidly than implied by the linear variation in Eq. (6). When these conditions are not met, the theoretical central intensities of the emission profiles end up systematically lower than the observed intensities, which makes it impossible to interpret the observations with this model.

2. When the conditions given in section (1) are met, the model interpretation of the observed E components of the H α and H β profiles yields the following estimates:

(a) $N_o \sim 10^{12} \text{ cm}^{-3}$; (b) the variations in N_o over a time scale of a few days range from 30 to 50% of the initial value; and, (c) the values of r_m range from 12 to $22R_o$. Typical examples of the theoretical differential profiles are compared

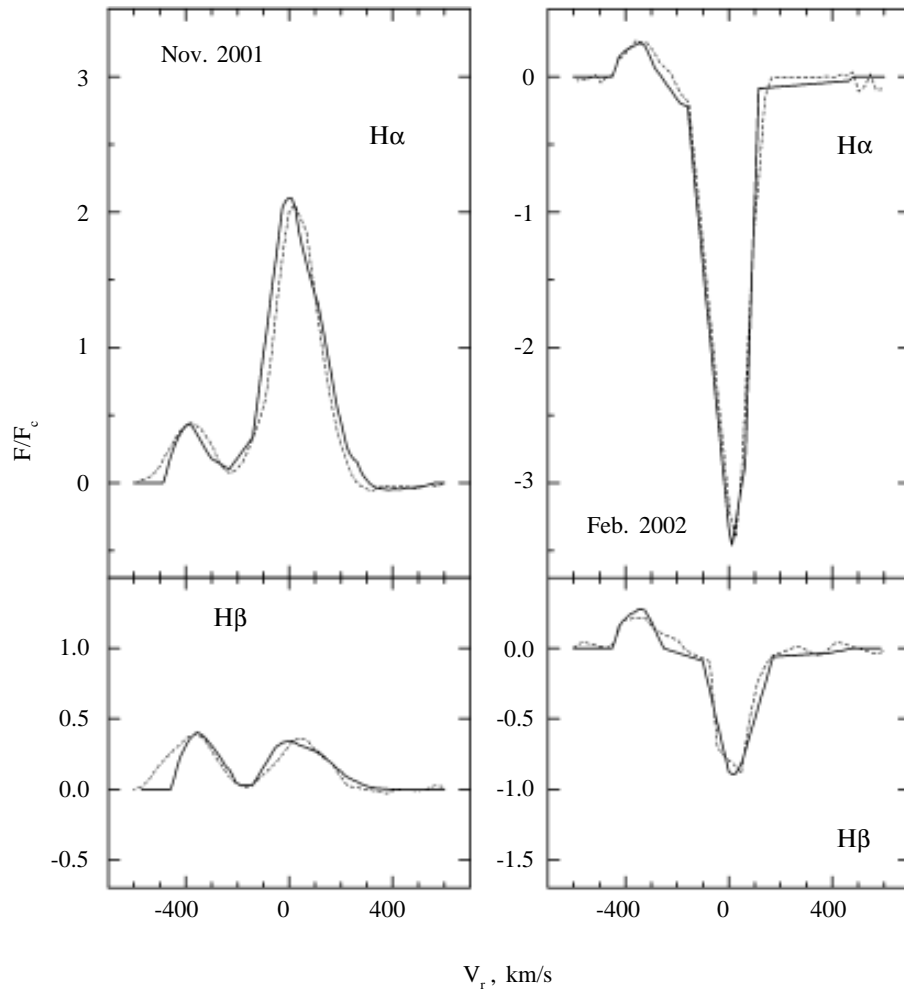


Fig. 6. Theoretical differential profiles of the H α and H β lines calculated for each observational season (Nov. 2001 and Feb. 2002). The observed differential profiles are shown for comparison as dotted curves (see Fig. 3, bottom). The following sets of model parameters were used in the calculations: $r_m = 12R_o$, initial density $N_o = 1.3 \cdot 10^{12} \text{ cm}^{-3}$, final density $N_o = 2.5 \cdot 10^{12} \text{ cm}^{-3}$ (Nov. 2001); $r_m = 12R_o$, initial density $N_o = 2.8 \cdot 10^{12} \text{ cm}^{-3}$, final density $N_o = 4.0 \cdot 10^{12} \text{ cm}^{-3}$ (Feb. 2002). The function $\Phi(r)$ was specified in accordance with Eq. (6).

with the observations (see Fig. 3, lower frame) in Fig. 6. In these models it is assumed that r_m is constant and the variation occurs because of changes in the initial density N_o of the stellar wind. The function $\Phi(r)$ is specified in accordance with Eq. (6).

3. The geometry and kinematics of the active region, as well as the above estimate of N_o , also yield an estimate for the rate of outflow of matter within the active wind on the order of $10^{-7} M_\odot$ per year and for its variation over a few days on the order of $3 \div 5 \cdot 10^{-8} M_\odot$ per year.

But it is still impossible to exclude a variant in which the active region is not as extended in latitude ($\text{tg}\varphi_1 > 0.1$) with φ_2 increasing with distance more rapidly than Eq. (6), and the initial density $N_o < 10^{12} \text{cm}^{-3}$. In this case, we have to recognize that explaining the observed variability in the maximum intensities of the $\text{H}\alpha$ and $\text{H}\beta$ emission lines in the spectrum of MWC 419 will also require that phenomena occurring beyond the confines of the above active region of the stellar wind will have to be taken into account.

9. Conclusion

Our spectroscopic data reveal a variability of the $\text{H}\alpha$ and $\text{H}\beta$ line profiles in the spectrum of the Herbig B8e star MWC 419 which is typical of Herbig Ae/Be stars with P Cyg line profiles. The main types of variation of these lines are the transformation of the profiles from type P CygII to P CygIII, and the reverse, as well as a change in the intensity of the overall emission in the line. In some case the P Cyg profiles acquire a more complicated form with two blue absorption components. The equivalent widths of the Balmer emission lines in the spectrum of this object are anomalously large compared to other stars of this subgroup. According to Böhm and Catala [27] the mass of the object is $5.2 M_\odot$ and its temperature is $T_{\text{eff}} = 11300 \text{K}$. According to the evolutionary scheme of Palla and Stahler [28], this star should be very young and lie essentially on the "birth line." In the future, before emerging onto the main sequence, its temperature should rise to 16000-17000 K, and it should become an early Be star. Young objects such as MWC 419 should have especially massive and elongated shells; this may be the reason for the strong line emission in its spectrum.

Our photometric measurements confirm that axis of the rotation of this object is inclined to the line of sight at an intermediate angle and are consistent with earlier observations by others.

The changes in the $\text{H}\alpha$ and $\text{H}\beta$ profiles in the spectrum of MWC 419, specifically their conversion over a few days from P CygII to P CygIII accompanied by a change in the total intensity of the lines, have been interpreted quantitatively using a differential model technique for two observational seasons, in November 2001 and February 2002. This showed that the observed variability can be explained in terms of a latitudinal redistribution of the density of the outflowing matter with a common change in the initial density at its base. In the active region the initial density of the gas at the base of the wind may approach 10^{12}cm^{-3} and vary by almost a factor of two over a few days (assuming that the outer radius of the shell r_m is $12R_o$) or by 20-30% (for r_m on the order of $20R_o$).

An estimate of the rate of outflow of matter in the active region shows that the rate of outflow may be $10^{-7} M_\odot$ per year, while it varies by $3 \div 5 \cdot 10^{-8} M_\odot$ over a year. For UX Ori variables, young stars with a mass on the order of $2.5 M_\odot$ and an age approaching that for the main sequence, disk wind models predict an overall rate of mass loss on the

order of $10^8 M_{\odot}$ per year [29]. Given that MWC 419 is a much more massive and younger star which has only recently departed from the "birth line," its stellar wind may be far more intense. Hence, our estimate of the rate of mass outflow for the active region of the stellar wind of MWC 419 is entirely plausible.

Calculations show that a magnetic field can control the kinetics of circumstellar gas and be one of the main mechanisms for accelerating the stellar wind in the region extending outward from the star's surface by $1-2R_*$. Assuming equality of the densities of magnetic and kinetic energy at the boundary of this zone, the required strength of the magnetic field is estimated to be 70 to 150 G. This estimate is fully consistent with direct measurements of the magnetic field at the base of the wind in a number of Herbig Ae/Be stars by Hubrig et al. [22]. Pogodin [18] has shown that for the typical outflow velocities in the stellar wind of Herbig Ae/Be stars (400-500 km/s), complete formation of a stellar wind zone after latitudinal redistribution of its density in its base region can take place over a few days. This time scale is consistent with the characteristic time of the spectral variability we have observed.

We have used an obviously simplified model in this study. In reality, during latitudinal redistribution of the density of the outflowing matter associated with a change in the structure of the magnetic field, we should expect the parameter r_a (an indicator of the efficiency of the effect of the field on the wind parameters) to vary as well as the density of the wind. However, further observational data are required in order to develop a more detailed model.

It should be emphasized that the results presented in this paper are just one of the possible ways of interpreting the spectral variability observed in MWC 419. Despite the simplicity of our model, many of the results obtained here appear to be quite universal. Thus, for example, the weak dependence of the differential theoretical profiles of the H α and H β lines in the P Cyg absorption region on the overall geometric structure of the wind region (except for the point where it intersects the line of sight), mean that our estimates of the parameters r_a and ρ_0 are applicable to a model for a wind that is not emerging from the star itself, but from a circumstellar disk. Future studies of this interesting object offer the possibility of verifying the correctness of our model, as well as of examining alternative variants of the model interpretation.

Organizing a program of polarimetric observations might make it possible to study the expected azimuthal inhomogeneity of the wind and the formation of dense jets within it. In the early stages of evolution before the main sequence, the level of activity in the circumstellar medium should be especially high. It would also be desirable to carry out a detailed spectroscopic study of this object with high spectral resolution and over a wider range of wavelengths.

We thank V. P. Grinin, S. A. Lamzin, and A. F. Kholtygin for useful comments on the differential model technique.

REFERENCES

1. G. H. Herbig, *Astrophys. J. Suppl. Ser.* **4**, 337 (1960).
2. L. A. Hillenbrand, S. E. Strom, F. J. Vrba, and J. Keene, *Astrophys. J.* **397**, 613 (1992).
3. U. Finkenzeller and R. Mundt, *Astron. Astrophys. Suppl. Ser.* **55**, 108 (1984).
4. V. P. Grinin and A. N. Rostopchina *Astron. zh.* **73**, 194 (1996).
5. N. G. Beskrovnyaya and M. A. Pogodin, *Astron. Astrophys.* **414**, 955 (2004).
6. M. A. Pogodin, G. A. P. Franco, and D. F. Lopes, *Astron. Astrophys.* **438**, 239 (2005).

7. M. A. Pogodin, Herbig Ae/Be Stars: High resolution spectroscopy and the structural-kinematic features of their shells [in Russian], Doctoral Dissertation, St. Petersburg (2001).
8. V. G. Kornilov and A. V. Mironov, Trudy GAISH 63, 400 (1991).
9. J. R. Ducati, Catalogue of stellar photometry in Johnson's 11 colour system, *Dept. of Astronomy*, University of Wisconsin (2002).
10. A. V. Kurchakov and F. K. Rspaev, Izvestiya MONRK 2(224), 31 (2002).
11. A. V. Kurchakov and F. K. Rspaev, Izvestiya MONRK 4(236), 32 (2004).
12. V. P. Grinin, N. N. Kiselev, and N. H. Minikulov, *Astrophys. Space Sci.* **186**, 283 (1991).
13. V. P. Grinin, P. S. Thé, D. de Winter et al., *Astron. Astrophys* **292**, 165 (1994).
14. V. S. Shevchenko, Herbig Ae/Be Stars [in Russian], Izd-vo "FAN," Tashkent, p. 51 (1989).
15. M. Fernández, *ASP Conf. Ser.* **62**, 51 (1994).
16. C. S. Beals, *Publ. Dom. Astron. Observ.* **9**, 1 (1951).
17. N. G. Beskrovnaya, M. A. Pogodin, R. V. Yudin et al., *Astron. Astrophys. Suppl. Ser.* **127**, 243 (1998).
18. M. A. Pogodin, Pis'ma v Astron. zh. 18, 1066 (1992).
19. N. G. Beskrovnaya, M. A. Pogodin, I. D. Najdenov, and I. I. Romanyuk, *Astron. Astrophys.* **298**, 585 (1995).
20. D. Mihalas and P. S. Conti, *Astrophys. J.* **235**, 515 (1980).
21. M. A. Pogodin, *Astrofizika* 32, 371 (1990).
22. S. Hubrig, R. V. Yudin, M. S. Shöller, and M. A. Pogodin, *Astron. Astrophys.* **446**, 1089 (2006).
23. L. V. Tambovtseva, V. P. Grinin, and O. V. Kozlova, *Astrofizika* **42**, 75 (1999).
24. V. V. Sobolev, Moving Shells of Stars [in Russian], Izd-vo. LGU, Leningrad (1947).
25. M. A. Pogodin, *Astrofizika* **24**, 491 (1986).
26. M. A. Pogodin, *Astrofizika* **31**, 150 (1989).
27. T. Böhm and C. Catala, *Astron. Astrophys.* **301**, 155 (1995).
28. F. Palla and S. W. Stahler, *Astrophys. J.* **418**, 414 (1993).
29. L. V. Tambovtseva, V. P. Grinin, B. Rodgers, and O. V. Kozlova, *Astron. zh.* **78**, 514 (2002).